A&A 463, 969–974 (2007)
DOI: 10.1051/0004-6361:20066014

Astronomy & Astrophysics

The properties of carbon stars found in the Byurakan and the Hamburg/ESO surveys⋆,⋆⋆

N. Mauron[1], K. S. Gigoyan[2], and T. R. Kendall[3]

[1] Groupe d'Astrophysique, CNRS and Univ. de Montpellier, CC 072, Place Bataillon, 34095 Montpellier Cedex 5, France
e-mail: nicolas.mauron@graal.univ-montp2.fr
[2] 378433 Byurakan Astrophysical Observatory and Isaac Newton Institute of Chile, Armenian Branch, Ashtarak d-ct, Armenia
[3] Centre for Astrophysics Research, Science and Technology Research Intitute,University of Hertfordshire, College Lane, Hatfield AL10 9AB, UK

Received 11 July 2006 / Accepted 30 October 2006

ABSTRACT

Aims. We analyse two samples of high latitude carbon stars found in two objective-prism surveys: the First Byurakan survey (FBS) and the Hamburg/ESO survey (HES). We determine the composition of these samples in cool AGB stars, warmer giants and dwarf carbon stars.
Methods. We list 44 new carbon stars found in the FBS and use near-infrared photometric catalogues (DENIS, 2MASS) to investigate the observational and statistical properties of the surveys. The SuperCOSMOS and USNO-B1.0 catalogues are used to study proper motions and to identify dwarfs.
Results. The colour–magnitude and colour–colour diagrams, either with visual magnitudes or with infrared data, show that the HES selects faint and relatively warm carbon stars, whereas FBS is less deep, but gives cooler objects. By comparing DENIS and 2MASS photometry, we find that HES objects with $J - K \leq 1$ are mostly non-variable giants while clear variability is often seen for $J - K \geq 1$, indicating AGB stars. By using SuperCOSMOS proper motions, 9 HES objects are found to have a proper motion μ greater than 30 mas yr^{-1} (3σ detection). Five of these objects are detected at the $\geq 5\sigma$ level. These 9 HES objects are dwarf carbon stars, including two that could belong to the halo population. The 9 carbon dwarfs are remarkably bright and deserve further study.

Key words. stars: carbon – surveys – Galaxy: halo – Galaxy: stellar content

1. Introduction

Carbon (C) stars are known to be of various types and origins. For example, they may be very cool and dusty giants evolving on the asymptotic giant branch (AGB) where the excess of carbon present in their atmospheres results from nucleosynthesis in the stellar interior. They can also be binary stars, often warmer giants or even dwarfs having gained carbon-rich material by accretion from a more evolved companion (for a review of C stars, see Wallerstein & Knapp 1998).

The faint C stars located at high galactic latitude and/or far from the galactic plane are of special interest because, if they are found to be giants or AGB stars, they do not belong to the galactic disk, in contrast to the large majority of catalogued C stars. A number of methods have been used to discover these high latitude C stars. One method consists of selecting candidate stars through their photometric colours and performing follow-up spectroscopy. Using this method, Totten and Irwin (1998) selected very red objects in the APM photometric catalogue (from digitized Schmidt plates, Irwin 2000) over an area of 6500 deg^2. A similar search was carried out by Mauron et al. (2004, 2005) where candidate C stars were selected by their photometric colours in the 2MASS point-source catalogue (Skrutskie et al. 2006) and with $|b| > 20°$. Together, these works identified ∼130 cool AGB C stars located in the halo and with distances up to 130 kpc. Another recent survey for faint high latitude C stars is that of Downes et al. (2004) who selected their candidates over an area of 3000 deg^2 by using Sloan Digital Sky Survey (SDSS) photometry. They discovered 251 relatively faint objects ($R > 16$), with a number of warm C giants and at least 110 dwarf C stars confirmed by their proper motions.

A very different but equally efficient method to discover C stars is to carry out objective prism spectroscopy. Early surveys designed to find C stars at high galactic latitude include the Case survey by Sanduleak & Pesch (1988) covering ∼1000 deg^2 in the north galactic cap, and the University of Michigan Thin prism Survey of MacAlpine & Lewis (1978) covering ∼225 deg^2 in the south cap. These surveys yielded 28 C stars (Bothun et al. 1991).

In this work, we examine the results of two more extended objective prism surveys that avoid the galactic plane. One is the First Byurakan Survey (FBS) with first results on C stars reported in Gigoyan et al. (2001; hereafter Paper I). The other is the Hamburg/ESO Survey (HES) described by Wisotzki et al. (2000). Christlieb et al. (2001) used the database of this survey for a search for stars with strong C_2 and/or CN lines. Our goal is to investigate the properties of these two surveys, and to determine their contents in AGB stars and dwarf carbon stars.

⋆ Partly based on observations done at ESO, Chile (program 69.B-0086), at Byurakan Observatory (Armenia), and at Haute Provence Observatory (France) operated by the Centre National de Recherche Scientifique.

⋆⋆ Appendices and Table 1 are only available in electronic form at http://www.aanda.org

2. The FBS and HES surveys

The First Byurakan Sky Survey covers 17 000 deg^2. According to Mickaelian et al. (2005), its magnitude limit in the V band is ∼17.5, but the C stars discovered in this survey are brighter than this limit (see Sect. 4.1). The objective prism FBS plates have a size of 4° × 4° and a large spectral range (3400–6900 Å). The dispersion is 2500 Å mm^{-1} near Hβ and the spectral resolution is on average ∼50 Å. For the search for C stars, this survey has been exploited so far by visual inspection. C stars are identified via the presence of C_2 bands. From the examination of an area of ∼6140 deg^2, 35 C stars were discovered and analysed by Gigoyan et al. (2001).

The Hamburg/ESO survey for C stars covers 6400 deg^2 limited by $\delta < +2.5°$ and $|b| > 30°$. All the plates were digitized and the magnitude limit is $V \sim 16.5$. The individual spectra have a wavelength range of 3200 to 5200 Å and a typical resolution of 15 Å at Hγ. Christlieb et al. (2001) searched for C stars by applying an automated procedure to the digitized spectra, and found a total of 403 faint high latitude C stars in this survey.

3. New carbon stars from the FBS

We consider a list of 44 additional C stars found in the FBS survey (Table 1). These 44 C stars were published by Gigoyan et al. (2006), and we give here complementary information not presented in that paper, particularly the coordinates of the objects, and a discussion of the adopted absolute magnitudes. The 44 C stars listed in Table 1 were found in regions of the sky which had not been inspected previously. The table in Appendix A provides the characteristics of the zones that were examined and their areas. The total area of these zones is 9755 deg^2. Slit spectroscopy of FBS C stars has been performed to confirm their carbon-rich nature. All observed objects were found to be carbon rich. Details of the instrumental configuration, as well as figures of the spectra obtained, can be found in the online Appendix. Two representative low resolution spectra are shown in Fig. 1.

Almost all stars classified as N-type from the FBS plate spectra or from the follow-up spectroscopy were found to have a 2MASS colour of $J - K > 1.4$. The only exception is one object (#68). For these red stars, distances in Col. 10 of Table 1 were estimated from their K magnitude and $J - K$ colour index. For a given $J - K$ index, an average absolute K-band magnitude was derived by considering LMC C stars as templates, and by assuming a distance modulus $m - M = 18.50$ for the LMC. These absolute magnitudes are found to be typically between −7.4 and −7.9. The dispersion of these values is of the order of 0.4–0.5 mag.

Concerning the C stars that are not N-type, the $J - K$ index typically lies between 0.6 and 1.0. For these colours, the scatter of K magnitudes for C stars in the LMC is too large to be used as a luminosity indicator of these stars. The low-resolution slit spectra that have a sufficiently good signal-to-noise ratio show that, in many cases, there is a strong CH-band at 4300 Å. In principle, these objects could be CH-type C stars. In the absence of data concerning their metal abundances, proper motions and radial velocities, we cannot exclude that some objects are R-type. The spectroscopic differences between these two classifications can be very subtle and practically invisible in our spectra (see for example Fig. 2 of Goswami 2005). Here, we make the simplifying hypothesis that all stars with $J - K < 1.2$ are CH-type.

In their Table 4, Totten and Irwin (1998) take $M_R = -3.5$ for both N-type and CH-type stars, but they note that CH-type are intrinsically somewhat fainter. In fact, CH stars have a range of luminosities, from $M_V \sim -2$ at the top of the red giant branch like the CH stars in ω Centauri, down to $M_V \sim +4$ on the subgiant branch (Wallerstein & Knapp 1998). A high luminosity will be assumed here. As the mean colour $V - R$ of this kind of high latitude warm C star is ∼0.6 ($\sigma = 0.5$), as measured for the HES stars, we adopted $M_R = -2.5$. Distances quoted in Table 1 were derived after taking into account interstellar extinction derived from the maps of Schlegel et al. (1998).

There are large uncertainties in these distances, both for N-type and other objects, at least ±25%. It can be seen that N-type stars (sources with $J - K > 1.2$) have distances up to 16 kpc from the Sun, and heights from the galactic plane of up to 12 kpc. For warmer objects, the range in distance is slightly lower (13 kpc), provided our choice of absolute magnitude is correct.

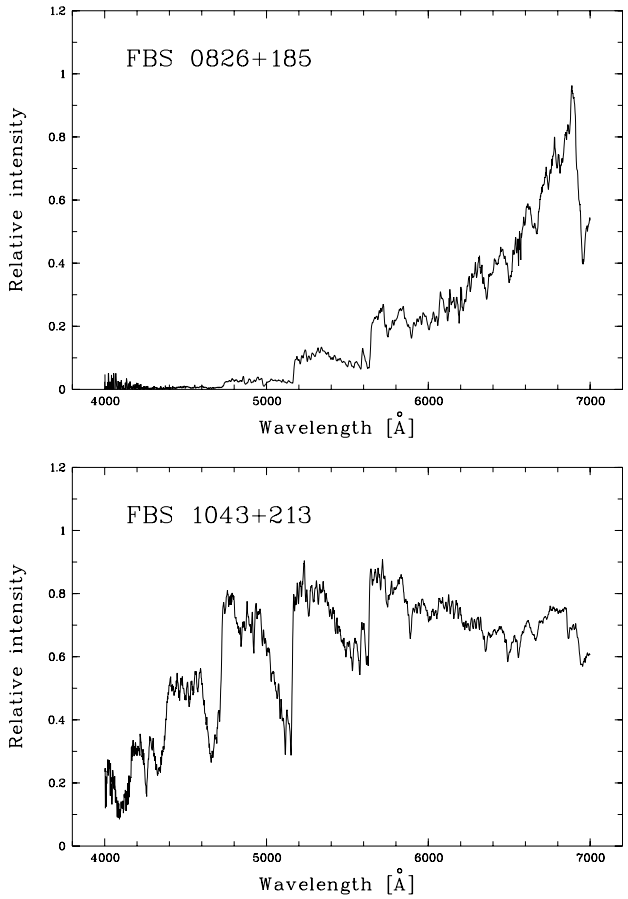

Fig. 1. Two representative low resolution spectra obtained at Byurakan Observatory. In the upper panel, the object is FBS 0826+185, a cool N-type star with $R = 11.5$, $B - R = 4.6$, $J - K = 1.68$ and $b = +30°$. In the lower panel, the object is FBS 1043+213, a warm C star with $R = 11.2$, $B - R = 2.3$, $J - K = 0.88$ and $b = +61°$.

4. Properties of the FBS and HES samples

4.1. Visible photometry

Here, we examine the R-band magnitude and $B - R$ colour index for the 79 FBS C stars, and make a comparison with the C stars from the HES survey. These R and B magnitudes are from the USNO-A2.0 catalogue in the great majority of cases. The accuracy of this visible photometry is of the order of ∼0.4 mag.

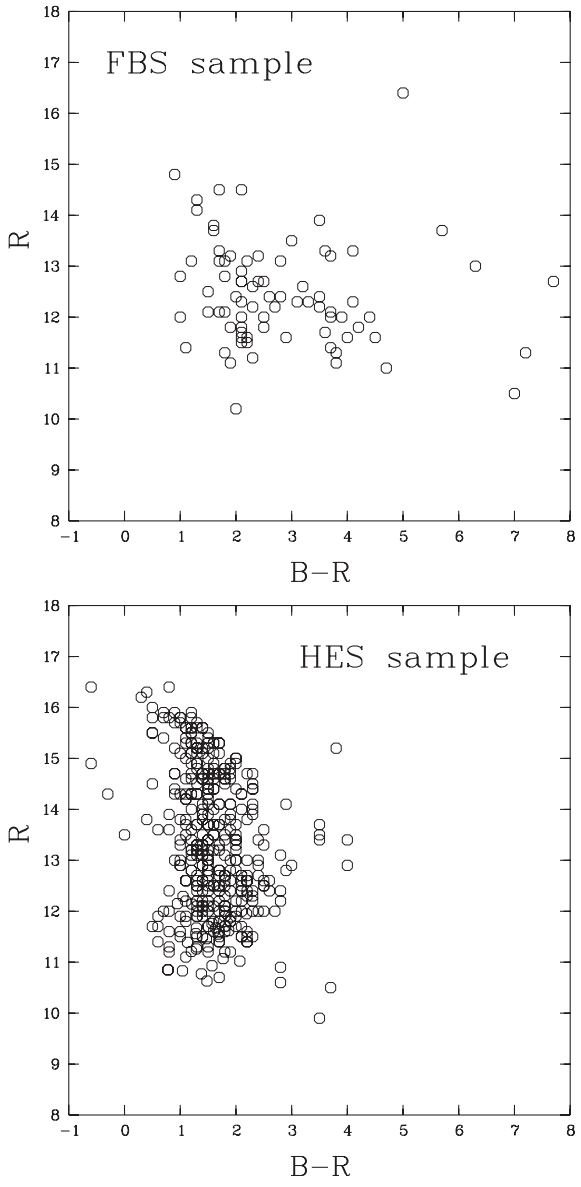

Fig. 2. Plots of the R-band magnitude as a function of the $B-R$ colour index. *Upper panel*: FBS objects from Paper I and this paper. *Lower panel*: HES objects.

In Fig. 2, upper panel, one can see that most of the 79 FBS stars have R between 11 and 14.5. One star has $R = 16.4$. For this star, FBS 1502+359 (Paper I), R is from the APM catalogue because no USNO-A2.0 R or B magnitude was available. This very red object may be a variable observed at a magnitude brighter than $R = 16$ when the FBS plate was exposed. Therefore, the faintest R magnitude for FBS stars appears to be $R \sim 14.5$. The FBS stars range from $B-R \sim 1$ up to $B-R \sim 6$–7, i.e., very red stars can be detected.

The lower panel of Fig. 2 presents the same R vs. $B-R$ diagram for the HES survey. Most of the stars have R between 11 and 16, showing that the HES survey is about 1.5 mag deeper in R than the FBS. For example, it is found that in the FBS sample 7% have $R > 14$, compared with 33% for the HES survey. Concerning the colours, one sees that very few HES stars have $B-R > 3$ (2% of the sample); the corresponding number is 32% for the FBS.

Figure 2 also shows that, for a given magnitude range, common to both HES and FBS (for example R between 12 and 13), there is a considerably larger number of sources detected in the HES than in the FBS. This is not due to a limiting magnitude effect, but more probably to the superiority of automatic detection of carbon features compared to visual inspection. The densities of detected sources per square degree are ~0.06 for HES and only ~0.005 for FBS. The FBS plates have been digitized (Mickaelian et al. 2005; see also the web site `http://astro1.phys.uniroma.it/DFBS/fbs.htm`) and an automated search and classification of fainter C stars in the FBS should be feasible in the future.

4.2. 2MASS photometry

Photometry from 2MASS is available for all sources in our two samples (except one object in the HES). One advantage of 2MASS compared to USNO-A2.0 is its much greater photometric accuracy. For FBS sources, the errors on J and K are all less than 0.03 mag, except in one case. For HES sources, which can be fainter in J and K, the errors on J are lower than 0.04 mag for 98% of objects, and the error in K is lower than 0.06 mag for 98% of objects. A few cases, with K fainter than 14, have lower accuracies, although they are always smaller than 0.1 mag.

In the colour-magnitude diagram for the HES stars (Fig. 3, lower panel), one sees two populations, one with $J-K < 1$ that we interpret as warm (giant or dwarf) C stars, and a second one with $J-K > 1$. This last group comprises 29 objects (7% of the total), and we suggest that it is composed of optical (i.e., not very dusty) AGB C stars.

There are a few especially distant AGB stars in this last group, since there are 8 objects with $J-K > 1$ and $K \geq 10$. All lie at galactic latitude $|b| > 30°$. If one selects objects with $J-K > 1.2$ and $K > 10$, we find 3 objects. Two objects, HE 0207−0211 and HE 1442−0058, with distances ~30 and 40 kpc, were already known and listed in Totten and Irwin (1998). The third, HE 1344−0411, was unknown. It has the following characteristics: $K = 10.47$, $J-K = 1.24$, $b = +55°$. Based on the K-band luminosity of the LMC C stars having the same $J-K$, its absolute magnitude is $M_K \approx -7.0$. Consequently, its distance is about 30 kpc and its height above the galactic plane is ~25 kpc.

Figure 3, upper panel, shows the colour–magnitude diagram for FBS stars. There are 36 objects with $J-K > 1$, representing 46% of the total sample. In the FBS sample, none of the stars with $J-K > 1$ reaches $K = 10$ because the FBS survey is poorer in depth than the HES and misses C stars which are too faint. However, the FBS is able to detect very red stars with $J-K > 2$, while none are detected by the HES.

Figure 4 shows colour–colour diagrams with 2MASS data. The diagram of the FBS sample shows the three families of C stars that FBS can detect, i.e. warm C stars, optical AGB C stars with $J-K$ between 1 and 2, and very red AGB C stars with $J-K > 2$. The HES experiment did not detect any very red C stars. This is obviously due to its blue−visible spectral range. For example, HES missed 11 C stars listed in Mauron et al. (2004, 2005), although these objects satisfy $R < 16$, $b < -30°$ and $\delta < +2°$. The reason is that their $B-R$ colour is too large and the signal at blue wavelengths is too faint.

4.3. Variability

Because the HES objects lie at $\delta < +2.5°$, a significant fraction of them were seen in the DENIS southern infrared survey (Epchtein 1998; Epchtein et al. 1999). From the last DENIS release available at the CDS (Strasbourg), we found that of

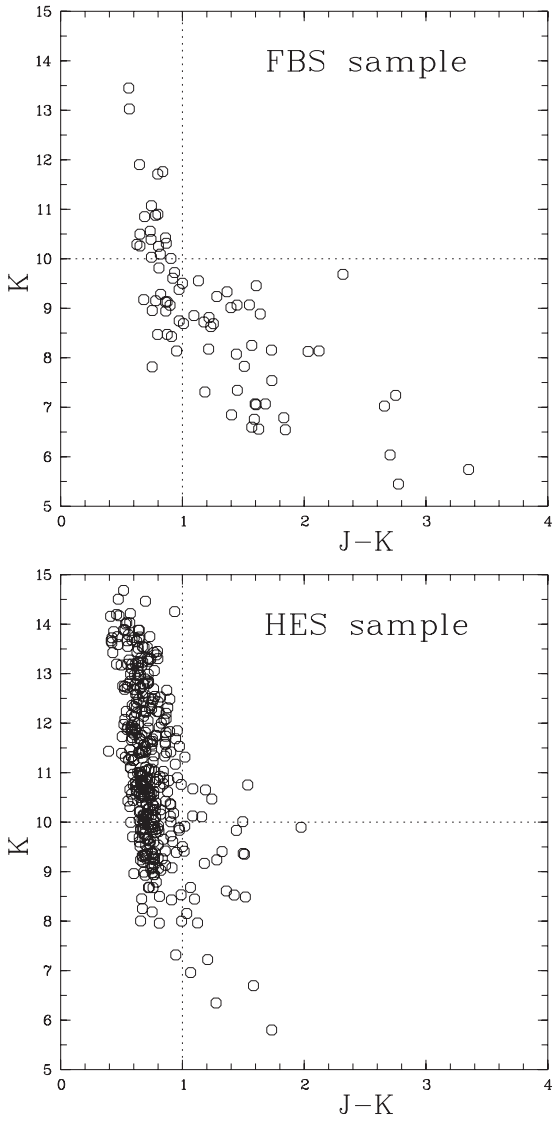

Fig. 3. Colour-magnitude diagrams K vs. $J-K$. *Lower panel*: HES sources. *Upper panel* : FBS sources. In both panels, the limits $J-K=1$ and $K=10$ are overplotted (see text).

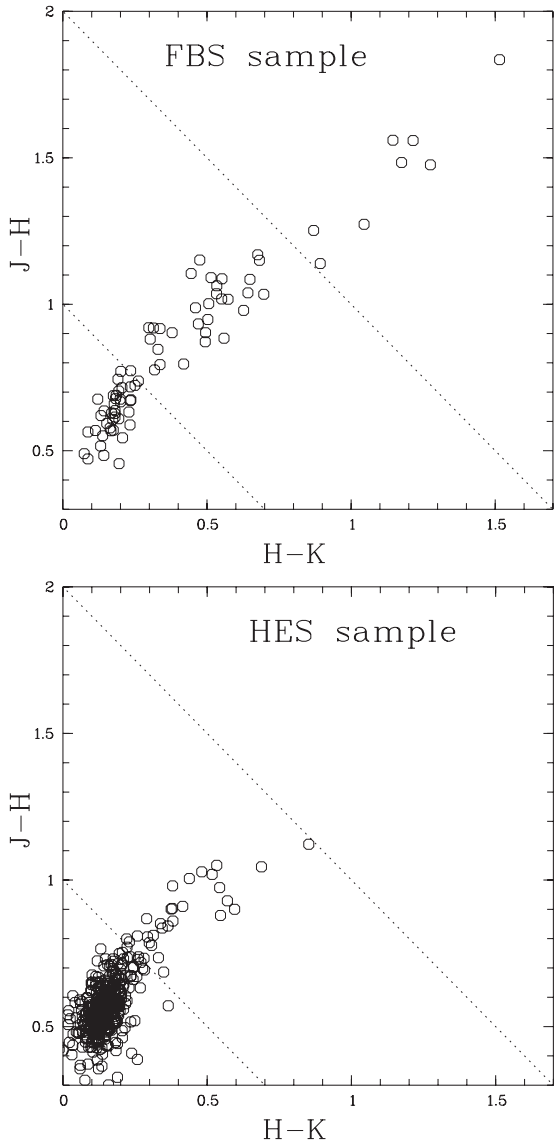

Fig. 4. Colour–colour diagrams with $J-H$ vs. $H-K$ (from 2MASS photometry). *Lower panel*: HES sources. *Upper panel*: FBS sources. In both panels, the dotted lines correspond to $J-K=1$ and $J-K=2$.

402 HES objects, 271 have DENIS data. The DENIS survey provides I, J, K-band photometry, so that one can compare Denis J and K with the 2MASS J and K observations in order to detect photometric variability. A direct comparison can be made because the transmission functions of these filters are very similar (see Fig. 4 of Bessel 2005), and because a quantitative analysis demonstrated no significant differences between the two photometries (Cabrera-Lavers & Garzon 2003, and references therein). The epoch differences between 2MASS and DENIS observations are scattered in the range 0 to 1500 days. In general, the measurement uncertainty on K is larger than in J, so we limit our investigation to the J-band.

Figure 5 shows the difference $\Delta J = J_{\rm DENIS} - J_{\rm 2MASS}$ as a function of the 2MASS $J-K$ colour. It can be seen that for $J-K<1$, the majority of the objects have ΔJ close to zero. There is only one object at $J-K=0.71$ for which $\Delta J=0.63$, and this variation in J is supported by a similar although smaller variation in K ($\Delta K=0.37$). If we omit this variable object, for a subsample of 245 objects, the average of ΔJ is 0.005 mag, with an rms of 0.078 mag. Given the uncertainties on the DENIS and 2MASS photometry, a very large majority of stars in this subsample are thus stable in flux. In contrast, for the subsample formed by the 22 redder stars with $J-K>1$, ∼8 stars display variability, of up to about one magnitude. For these 22 objects, the average ΔJ is –0.10 with a dispersion of 0.34 mag.

Concerning the FBS survey (which covers only a fraction of the southern hemisphere), we found only 15 stars belonging to the DENIS survey, so that the statistics are poor. Only one source shows a significant flux variation between DENIS and 2MASS data. It is FBS 0846−071 ($\alpha = 08^{\rm h}49^{\rm m}10.96^{\rm s}$, $\delta = -7°21'44.24''$(J2000)), with $R=13.5$ and $B-R=3.0$ (see Paper I). Its variation is: $J_{\rm DENIS} - J_{\rm 2MASS} = 2.33$, and $K_{\rm DENIS} - K_{\rm 2MASS} = 1.99$. This star is a confirmed AGB C star with a distance of ∼17 kpc and a height from the galactic plane of ∼6 kpc.

4.4. Objects with proper motion

According to Christlieb et al. (2001), the HES sample may contain a small proportion of dwarf C stars. To investigate this point, we have searched for counterparts of the HES objects

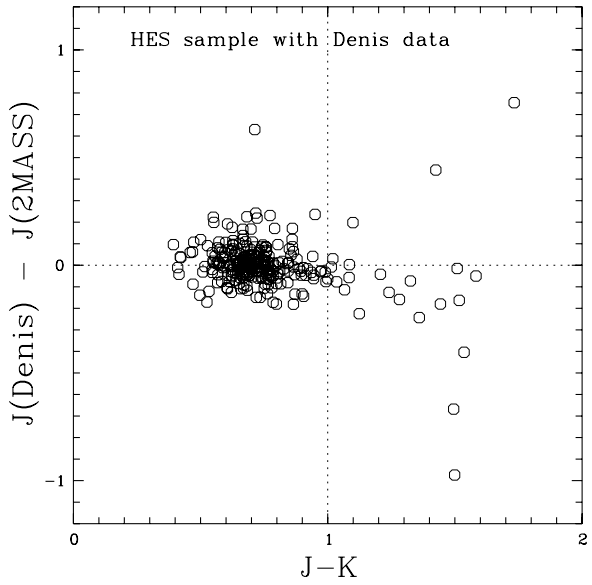

Fig. 5. Difference between J(DENIS) and J(2MASS) plotted as a function of the $J-K$ colour index of 2MASS.

in the SuperCOSMOS catalogue (Hambly et al. 2001a–c). SuperCOSMOS provides proper motions and their errors σ for the Southern hemisphere. These errors are of the order of 6 to 13 mas yr^{-1}. A total of 402 HES objects were found in SuperCOSMOS. Figure 6 shows μ_δ as a function of $\mu_\alpha \cos(\delta)$. Crosses have been overplotted when two conditions are met: the total proper motion must be above 30 mas yr^{-1} and at least in α or in δ one finds a $\geq 3\sigma$ detection. One sees that 9 sources satisfy these conditions and Table 2 provides the details of the SuperCOSMOS data. Table 2 also provides distances and tangential velocities, which will be discussed in the next section.

We have also searched for FBS objects with proper motions. We found only one with $\mu > 30$ mas yr^{-1}: it is FBS 0259+444 (listed in Paper I). The USNO-B1.0 catalogue of Monet et al. (2003) provides a rather high motion $\mu = 185$ mas yr^{-1} mainly in α. However, comparison of POSS images does not show any corresponding displacement, of the order of $\sim 7''$, for an interval of 38 years between examined plates. We noted instead that the star is blended with a fainter companion to the East, suggesting that the motion is an artefact.

5. Discussion

The accuracy of 2MASS photometry has allowed a clear separation of the HES objects into two groups. The objects with $J-K > 1$ are presumably AGB stars, an interpretation supported by the high fraction of variable stars in this group. There are no such objects with $K > 11$ because AGB stars as faint as this in K (and consequently very distant in the halo) are very rare, and are only found with specific methods (see, e.g. Mauron et al. 2004, 2005). We suggest that HES objects with $J-K < 1$ are red giant branch objects, or for a small fraction, dwarfs (see below). The giants are likely ordinary early R-type stars or CH-type C stars but high resolution spectroscopy is needed to separate the two types with certainty. Goswami (2005) obtained medium resolution ($\lambda/\delta\lambda \sim 1000$) spectra of 91 HES stars, and concluded the presence of 35 "potential candidate" CH stars.

On the (K, $J-K$) colour-magnitude diagram for HES objects, there is a clear tendency towards bluer $J-K$ colours with progressively fainter K magnitudes. At $K = 9$, $J-K$ is about 0.8, but at $K = 14$, $J-K$ is about 0.5 (Fig. 3). This trend is also visible for the FBS stars, although the statistics are much poorer. Joyce (1998) presented near-infrared spectroscopy of faint high latitude C (FHLC) stars. His spectra show that the J, H, and K bandpasses are dominated by CN, C_2 and CO molecular bands. While these bands are very strong for AGB stars with $J-K > 1$, they can nearly disappear for some FHLCs like CLS 26 and CLS 80 for which $J-K \approx 0.50$ (Joyce 1998). In that case the spectra are close to a smooth continuum decreasing with λ. Therefore, we suggest that this colour-magnitude trend indicates that bright objects have more pronounced molecular bands in JHK than faint objects. A possible explanation is that faint objects are on average more distant and probe populations (thick disk, halo) where the mean metallicity is lower, the giants on average hotter, and consequently the molecular bands fainter.

The fact that a few (9) HES sources have measurable proper motions is most noteworthy. Christlieb et al. (2001) had predicted that 10–5 out of the 403 HES objects should be dwarf carbon stars (dCs), so that the agreement between their predictions and our findings is reasonable. A remarkable property of the HES dCs is their high apparent intensity. All are brighter than $R = 15$ and 5 are brighter than $R = 14$. These dCs are clearly brighter than those from the SDSS survey (Downes et al. 2004). In Table 2, we have also listed the K magnitude in order to compare our sample with the C dwarfs listed by Lowrance et al. (2003). These authors give in their Table 1 a list of all C dwarfs known at the time of their writing, and 5 of their objects have $K < 12.5$. In our sample, we also find 5 sources with $K < 12.5$, i.e. we double the number of bright dC targets especially suited to spectroscopic investigations.

In Table 2, we have also estimated distances for each C dwarf by adopting a K-band absolute magnitude $M_K = +6.3$. This M_K comes from the only three C dwarfs for which a parallax has been measured (see Table 1 of Lowrance et al. 2003, Note d). Distance estimates are in the range 100 to ~500 pc. This allows us to calculate the tangential velocity v_t in km s^{-1}. Most of our carbon dwarfs have v_t between 20 and 60 km s^{-1}, but two have a v_t of 120 km s^{-1}. If our distance estimates are correct, these two objects could be halo carbon dwarfs.

6. Conclusions

In this paper on carbon stars located far from the galactic plane, we have considered two objective-prism surveys and analysed their properties. Our main results are the following:

- A list of 44 new C stars in the FBS has been considered. Their distances from the Sun, and from the galactic plane, are up to ~15 kpc.
- The 2MASS colour–magnitude and colour-colour diagrams show that the HES contains at least two populations, one bluer and one redder than $J-K = 1$. The FBS can detect stars with very red colours ($J-K > 2$).
- When one compares 2MASS and DENIS data, the HES blue population shows no sign of variability, while the red one does. The red population is probably made of AGB stars, while the blue population contains mainly stars on the red giant branch.
- In the blue population, the faint stars have a mean $J-K$ lower than the bright stars. We propose that, on average, these faint stars come from more distant populations of lower metallicity (thick disc, halo) than the bright stars. At low metallicity, the giants are warmer, and the molecular bands in the JHK

Table 2. HES objects with significant proper motions in SuperCOSMOS. In the 3rd and 4th columns, the proper motions in α and δ, and their respective 1σ errors are given, in mas yr^{-1}. In Cols. (5) and (6), we have listed the ratios κ_1 and κ_2 between measurements and their errors. For at least one coordinate, these ratios κ have to be greater than 3. Column (7) is an R-band magnitude from SuperCOSMOS. Col. (8) is the K-magnitude from 2MASS. Col. (9) is the total proper motion in mas yr^{-1}. Column (10) is the distance in pc. Column (11) is the tangential velocity in km s^{-1}.

Name	Coordinates (J2000)	$\mu_\alpha \cos(\delta)$	μ_δ	κ_1	κ_2	R	K	μ	d	v_t
(1)	(2)	(3)	(4)	(5)	(6)	(7)	(8)	(9)	(10)	(11)
HE 0009−1824	00 12 18.5 −18 07 55	+33.9 ± 10.0	−17.5 ± 11.0	3.4	1.6	15.5	13.66	38	300	54
HE 0343−5714	03 44 11.8 −57 05 09	+38.3 ± 7.2	−41.9 ± 5.9	5.3	7.1	15.9	14.68	57	475	128
HE 0432−3128	04 34 06.7 −31 22 11	+86.5 ± 4.6	+39.1 ± 5.4	18.8	7.3	15.4	13.51	95	280	125
HE 0930−0018	09 33 24.6 −00 31 45	−62.1 ± 6.0	+37.5 ± 5.9	10.3	6.4	13.7	11.33	73	100	34
HE 1058−2228	11 01 21.8 −22 44 31	+5.7 ± 10.1	−46.9 ± 13.9	0.6	3.4	12.4	11.39	47	100	22
HE 1116−1628	11 19 03.9 −16 44 49	−23.5 ± 6.7	+29.8 ± 4.6	3.5	6.5	14.4	12.48	38	170	31
HE 1205−0417	12 07 51.7 −04 34 40	−15.2 ± 6.5	−70.0 ± 6.1	2.3	11.5	14.2	11.68	72	120	40
HE 1358−2508	14 01 54.9 −28 56 24	+43.8 ± 9.0	+1.0 ± 8.2	4.9	0.1	15.8	13.44	44	270	56
HE 2329−0716	23 31 54.9 −06 59 32	+54.2 ± 12.7	−3.7 ± 14.7	4.3	0.2	13.9	12.16	54	150	39

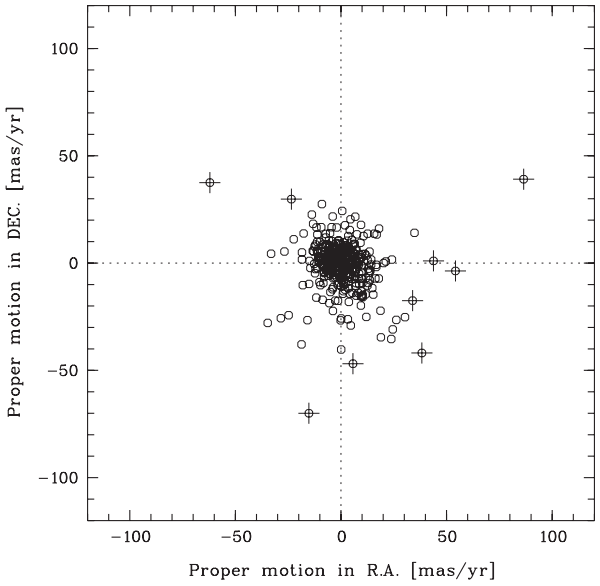

Fig. 6. Proper motions of 402 HES objects, with $\mu_\alpha \cos(\delta)$ in abscissa and μ_δ in ordinates. Circles with an overplotted cross correspond to cases where μ is larger than 30 mas yr^{-1} *and* where the motion in α or δ is detected with at least a $3\,\sigma$ quality.

filters are much less pronounced, and consequently the $J-K$ index becomes smaller.

– We investigated the proper motions of the HES stars by using the SuperCOSMOS data. We found 9 cases having detections at more than the $3\,\sigma$ level in α or δ, and with $\mu > 30$ mas yr^{-1}. These C dwarfs have an apparent brightness comparable to the brightest such cases presently known, and two objects could be halo C dwarfs.

Acknowledgements. We thank our referee, N. Christlieb, for several useful remarks. We also thank the people and organizations that were involved in the construction of the unique astronomical catalogues that were used in this research, particularly 2MASS, DENIS, USNO-B1 and SuperCOSMOS.

References

Bessel, M. S. 2005, ARA&A, 43, 293
Bothun, G. L., Elias J. H., MacAlpine, G., et al. 1991, AJ, 101, 2220
Cabrera-Lavers, A., & Garzon, F. 2003, A&A, 403, 383
Christlieb, N., Green, P. J., Wisotzki, L., & Reimers, D. 2001, A&A, 375, 366
Downes, R. A., Margon, B., Anderson, S. F., et al. 2004, AJ, 127, 2838
Epchtein, N. 1998, The impact of near-infrared surveys on galactic and extragalctic astronomy. Proc. 3rd. Euroconf., Kluwer ASSL, 230
Epchtein, N., Deul, E., Derriere, S., et al. 1999, A&A, 349, 236
Gigoyan, K., Mauron, N., Azzopardi, M., et al. 2001, A&A, 371, 560 (Paper I)
Gigoyan, K., Mickaelian, A. M., Mauron, N. 2006, Astrofizica, 49, 197
Goswami, A. 2005, MNRAS, 359, 531
Hambly, N. C., Mac Gillivray, H. T., Read, M. A., et al. 2001a, MNRAS, 326, 1279
Hambly, N. C., Irwin, M. J., & Mac Gillivray, H. T. 2001b, MNRAS, 326, 1295
Hambly, N. C., Davenhall, A. C., Irwin, M. J., & Mac Gillivray, H. T. 2001c, MNRAS, 326,1315
Irwin M. J. 2000, The APM Catalogue (the web site is `http://www.ast.cam.ac.uk/ apmcat/`)
Joyce, R. R. 1998, AJ, 115, 2059
Lowrance, P. J., Kirkpatrick, J. D., Reid, I. N., et al. 2003, ApJ, 584, L95
MacAlpine, G. M., & Lewis, D. 1978, ApJS, 36, 587
Mauron, N., Azzopardi, M., Gigoyan, K., & Kendall, T. R. 2004, A&A, 418, 77
Mauron, N., Kendall, T. R., & Gigoyan, K. 2005, A&A, 438, 867
Mickaelian, A. M., Hagen, H.-J., Sargsyan, L. A., et al. 2005, CDS catalog VI/116, Byurakan Observatory Publications (see also the web site `http://astro1.phys.uniroma1.it/DFBS/fbs.htm`)
Monet, D. G., Levine, S. E., Canzian, B., et al. 2003, AJ, 125, 984
Sanduleak, N., & Pesch P. 1988, ApJS, 66, 387
Schlegel, D. J., Finkbeiner, D. P., & Davis M. 1998, ApJ, 500, 525
Skrutskie, M. F., Cutri, R. M., Stiening, R., et al. 2006, AJ, 131, 1163
Totten, E. J., & Irwin M. J. 1998, MNRAS, 294, 1
Wallerstein, G., & Knapp, G. R. 1998, ARA&A 36, 369
Wisotzki, L., Christlieb, N., Bade, N., et al. 2000, A&A, 358, 77

Online Material

Table 1. New FBS carbon stars. Column 1: Running number following that given in Gigoyan et al. (2001). Column 2: FBS name. Columns 3 and 4: J2000 coordinates from 2MASS; Col. 5: Galactic coordinates; Cols. 6 and 7: R mag. and $B-R$ colour from the USNOC-A2.0 catalogue; Cols. 8 and 9: K mag and $J-K$ colour from 2MASS; Col. 10: distance estimate in kpc; Col. 11: estimate of the height in kpc above or below the galactic plane.

(1) No.	(2) FBS No.	(3) α(J) h m s	(4) δ(J) ° ′ ″	(5) l, b ° °	(6) R mag	(7) $B-R$ mag	(8) K mag	(9) $J-K$ mag	(10) d kpc	(11) z kpc
36	0318 + 238	03 21 16.3	+23 58 50	161 −27	10.2	2.0	7.82	0.75	2.5	−1.1
37	0502 + 088	05 05 00.2	+08 56 09	191 −18	12.7	7.7	6.04	2.71	5.0	−1.5
38	0520 + 029	05 23 02.3	+03 01 45	199 −18	12.3	3.3	6.76	1.59	8.0	−2.5
39	0707 + 270	07 10 47.9	+26 59 03	190 +16	11.3	7.2	5.45	2.77	4.0	+1.1
40	0707 + 310	07 10 48.3	+30 55 46	186 +17	11.0	4.7	6.60	1.57	7.5	+2.0
41	0729 + 269	07 32 32.7	+26 47 15	192 +20	11.7	3.6	8.16	1.73	16.0	+5.5
42	0731 + 274	07 34 23.9	+27 19 12	192 +21	12.0	4.4	7.54	1.73	12.0	+4.5
43	0826 + 185	08 29 15.1	+18 23 07	206 +30	11.5	4.6	7.07	1.68	10.0	+5.0
44	0826 + 109	08 29 29.0	+10 46 24	214 +27	13.0	6.3	8.14	2.12	16.0	+7.5
45	0900 + 034	09 03 15.7	+03 14 02	226 +31	12.1	1.7	9.13	0.88	8.0	+4.0
46	0904 + 213	09 07 12.0	+21 08 53	206 +39	11.6	2.1	8.96	0.75	6.5	+4.0
47	0916 + 029	09 18 50.8	+02 45 04	229 +33	11.4	1.1	8.47	0.80	6.0	+3.0
48	1043 + 213	10 46 05.9	+21 02 27	218 +61	11.2	2.3	8.47	0.88	5.5	+4.5
49	1043 + 253	10 46 38.6	+25 03 07	210 +62	13.1	1.8	9.72	0.93	13.0	+11.0
50	1140 + 038	11 42 49.1	+03 35 10	265 +61	12.0	1.0	9.18	0.68	8.0	+6.7
51	1145 − 000	11 47 59.7	−00 19 18	271 +58	12.4	2.8	10.01	0.91	9.0	+7.5
52	1152 − 039	11 55 06.1	−04 12 24	277 +59	11.5	2.2	8.43	0.91	6.0	+5.0
53	1225 + 077	12 27 40.4	+07 28 13	285 +69	13.1	1.7	10.85	0.68	13.0	+12.0
54	1238 − 046	12 41 33.2	−04 52 04	298 +58	13.1	1.2	11.07	0.75	13.0	+11.0
55	1305 + 015	13 08 17.7	+01 16 49	313 +67	12.2	2.3	9.81	0.81	8.0	+7.5
56	1406 + 027	14 09 00.7	+02 32 12	343 +59	12.8	1.0	10.39	0.74	11.0	+9.5
57	1418 − 031	14 20 57.2	−03 19 54	341 +52	12.0	2.5	9.51	1.00	7.5	+6.0
58	1418 + 018	14 21 01.2	+01 37 18	347 +56	11.8	1.9	9.13	0.86	7.0	+6.0
59	1440 + 263	14 42 48.4	+26 10 30	037 +65	12.4	2.6	9.06	0.90	9.0	+8.0
60	1451 + 075	14 53 33.7	+07 20 12	004 +55	11.7	2.1	9.38	0.97	7.0	+5.5
61	1516 + 151	15 18 40.2	+14 59 03	021 +53	11.1	3.8	7.34	1.45	10.0	+8.0
62	1524 + 046	15 27 23.6	+04 28 28	009 +46	12.0	3.9	8.13	2.03	16.0	+12.0
63	1547 + 046	15 49 52.6	+04 28 35	013 +42	12.2	2.4	9.79	0.75	8.0	+5.5
64	1552 − 002	15 54 46.0	−00 25 51	008 +37	11.3	1.8	9.15	0.78	5.0	+3.0
65	1553 + 119	15 55 43.6	+11 47 16	022 +44	12.4	2.0	10.56	0.74	9.0	+6.0
66	1609 − 058	16 12 08.6	−05 55 51	006 +31	12.3	2.1	8.75	0.97	6.0	+3.0
67	1612 + 262	16 15 03.4	+26 07 51	043 +45	13.1	2.2	10.90	0.80	12.0	+8.5
68	1615 − 048	16 18 17.1	−04 56 42	008 +31	12.6	2.3	8.63	1.23	8.0	+4.0
69	1619 + 160	16 21 29.4	+15 52 57	031 +40	11.8	2.5	8.85	1.09	7.0	+4.5
70	1715 + 172	17 17 29.3	+17 13 56	039 +28	12.2	2.7	10.03	0.75	8.0	+4.0
71	1728 + 216	17 30 53.7	+21 38 41	044 +27	11.1	1.9	8.14	0.95	5.0	+2.5
72	1756 + 226	17 58 15.6	+22 35 53	048 +21	12.0	3.7	8.07	1.44	14.0	+5.0
73	1825 + 272	18 27 10.2	+27 14 40	055 +17	12.1	1.5	10.50	0.65	7.0	+2.0
74	2029 + 101	20 31 51.8	+10 17 57	054 −17	11.8	2.1	8.69	1.01	6.0	−1.8
75	2100 + 123	21 02 49.9	+12 32 26	061 −22	12.7	2.4	8.72	1.18	9.5	−3.5
76	2107 + 109	21 09 59.0	+11 11 04	061 −24	13.2	2.4	9.01	1.40	13.0	−5.5
77	2158 + 197	22 01 17.5	+20 01 49	077 −27	12.5	1.5	10.29	0.63	9.0	−4.0
78	2203 + 198	22 05 43.8	+20 08 10	078 −28	13.2	1.9	10.31	0.87	13.0	−6.0
79	2217 + 100	22 19 58.5	+10 15 04	073 −37	13.3	1.8	10.25	0.80	13.0	−8.0

Appendix A: Limits of the area scanned to find the FBS objects of Table 1

Table A.1 gives details on the sky regions on which the objects of Table 1 were found. Column (1) is the FBS Zone number, Col. (2) is the area in square degrees, Col. (3) gives the limits in declination in degrees, and Col. (4) provides the limits in right ascension.

Table A.1. Coordinates of the FBS area surveyed for C stars.

Zone No.	Area deg^2	δ limits ° °	α limits h m h m
11	1242	$-07 < \delta < -03$	0 00–5 20
			8 40–16 20
			20 20–24 00
12	1055	$-03 < \delta < +01$	0 00– 5 20
			8 00–16 20
			20 20–24 00
13	1013	$+01 < \delta < +05$	0 00–5 20
			8 10–16 10
			20 20–24 00
14	921	$+05 < \delta < +09$	0 00–5 20
			8 20 –16 10
			21 20 –24 00
15	993	$+09 < \delta < +13$	0 00–4 00
			7 50–16 40
			20 25–24 00
16	885	$+13 < \delta < +17$	0 00–3 40
			7 50–16 40
			21 10–24 00
17	950	$+17 < \delta < +21$	0 00–3 20
			7 20–18 15
			22 00–24 00
18	935	$+21 < \delta < +25$	0 00–3 55
			7 00–18 20
			22 30–24 00
19	910	$+25 < \delta < +29$	0 00–3 00
			7 00–19 30
			22 40–24 00
20	851	$+29 < \delta < +33$	0 00–2 50
			7 00–18 20
			21 45–24 00

Appendix B: Confirmation spectroscopy of FBS carbon stars

In order to confirm the carbon-rich nature of FBS objects (including those of Paper I), follow-up slit spectroscopy has been carried out using various intrumental setups. These observations are often performed as backup programs of other projects. Not all FBS objects could be checked, but all observed sources were found to be carbon-rich. The utilised instruments are detailed below.

Spectra from 5700 to 6600 Å were obtained at Haute-Provence Observatory with the 1.93-m telescope with the Carelec spectrograph. This instrument was equipped with a 1200 lines mm^{-1} grating giving a dispersion of 0.45 Å pixel^{-1} on the detector, which was an EEV 2048 × 1024 chip, with pixels of 13.5 μm. The slit was 2″ and the final resolving power is $R \approx 3300$.

Spectra from 5800 to 8400 Å were obtained at the ESO Danish 1.5-m telescope equipped with the DFOSC focal reducer. Grism # 8 was used to give a dispersion of 1.2 Å pixel^{-1} on the EEV/MAT CCD 2148 × 4096 detector. The slit width was 1.5″ and the resolving power is $R \approx 2500$.

Low resolution spectra were taken at the 2.6-m telescope of Byurakan Observatory. The spectrograph had a grating of 600 lines mm^{-1}, providing a dispersion of 1.7 Å pixel^{-1} on a 2063 × 2058 CCD detector, with pixels of 15 μm. The final resolving power is $R \approx 700$.

On medium resolution spectra, molecular bands typical of carbon stars can be seen at 6130 and 6190 Å (due to C_2), and at 6925 and 7850 Å (due to CN). On low resolution spectra, the C_2 bands are obvious.

The attached figures concern the following objects:

a) from Paper I, 9 further objects are confirmed (in addition to the 22 objects that had been confirmed in Paper I): FBS 0137+400, 0518+687, 0644+616, 0846−071, 0922+786, 1431−079, 1618−087, 2123−104, 2207−095.

b) from this paper Table 1, 24 objects are confirmed. At medium resolution: FBS 0318+238, 0502+088, 0520+029, 2029+101, 2100+123, 2107+109, 2203+198, and 2217+100. At low resolution: FBS 0318+238, 0502+088, 0707+270, 0707+310, 0729+269, 0731+274, 0826+109, 0826+185, 0900+034, 1043+213, 1043+253, 1225+077, 1305+015, 1524+253, 1524+046, 1553+119, 1756+226, 1825+272, 2158+197.

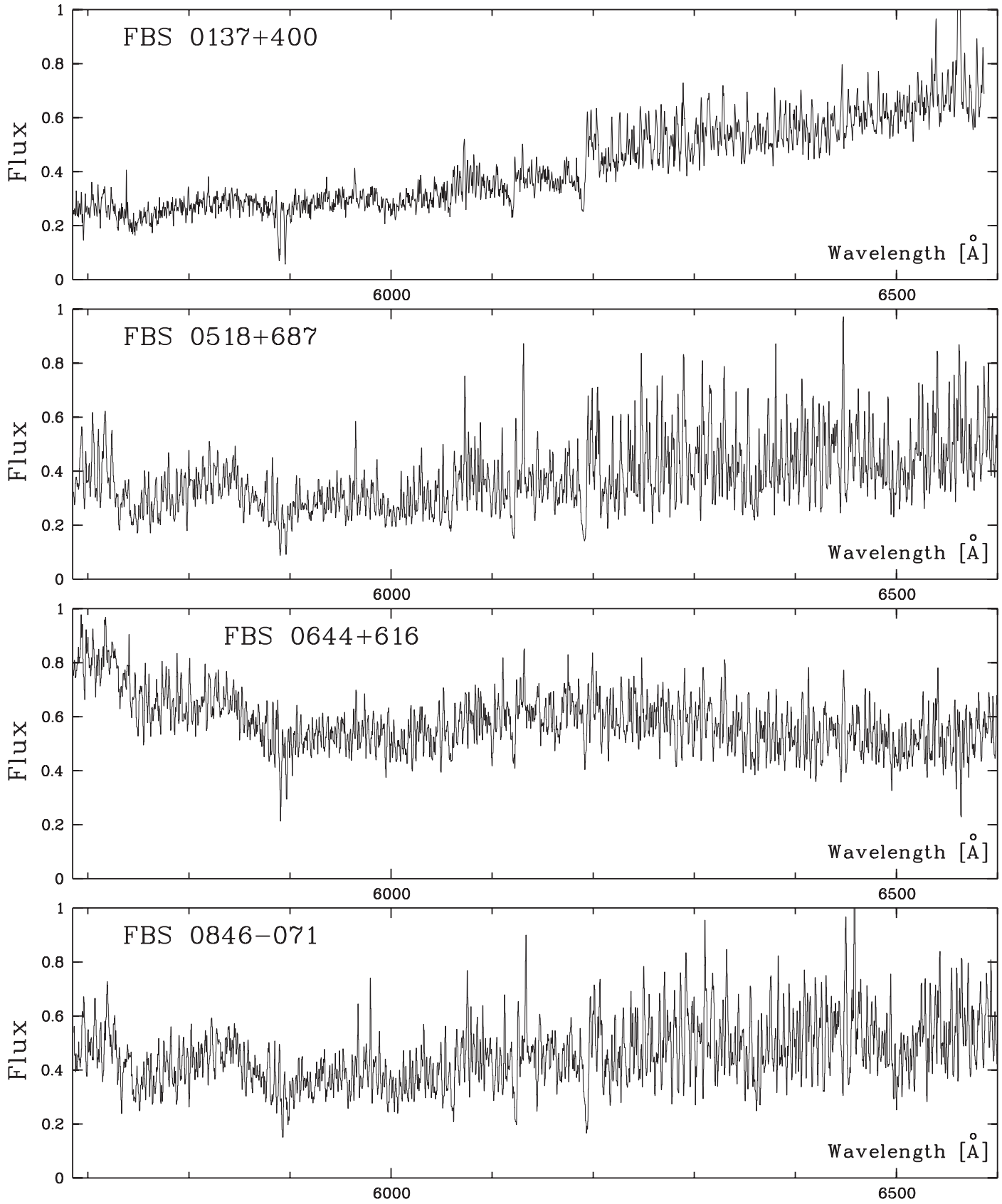
FBS 0137+400
FBS 0518+687
FBS 0644+616
FBS 0846−071
Flux
Wavelength [Å]
0
0.2
0.4
0.6
0.8
1
6000
6500

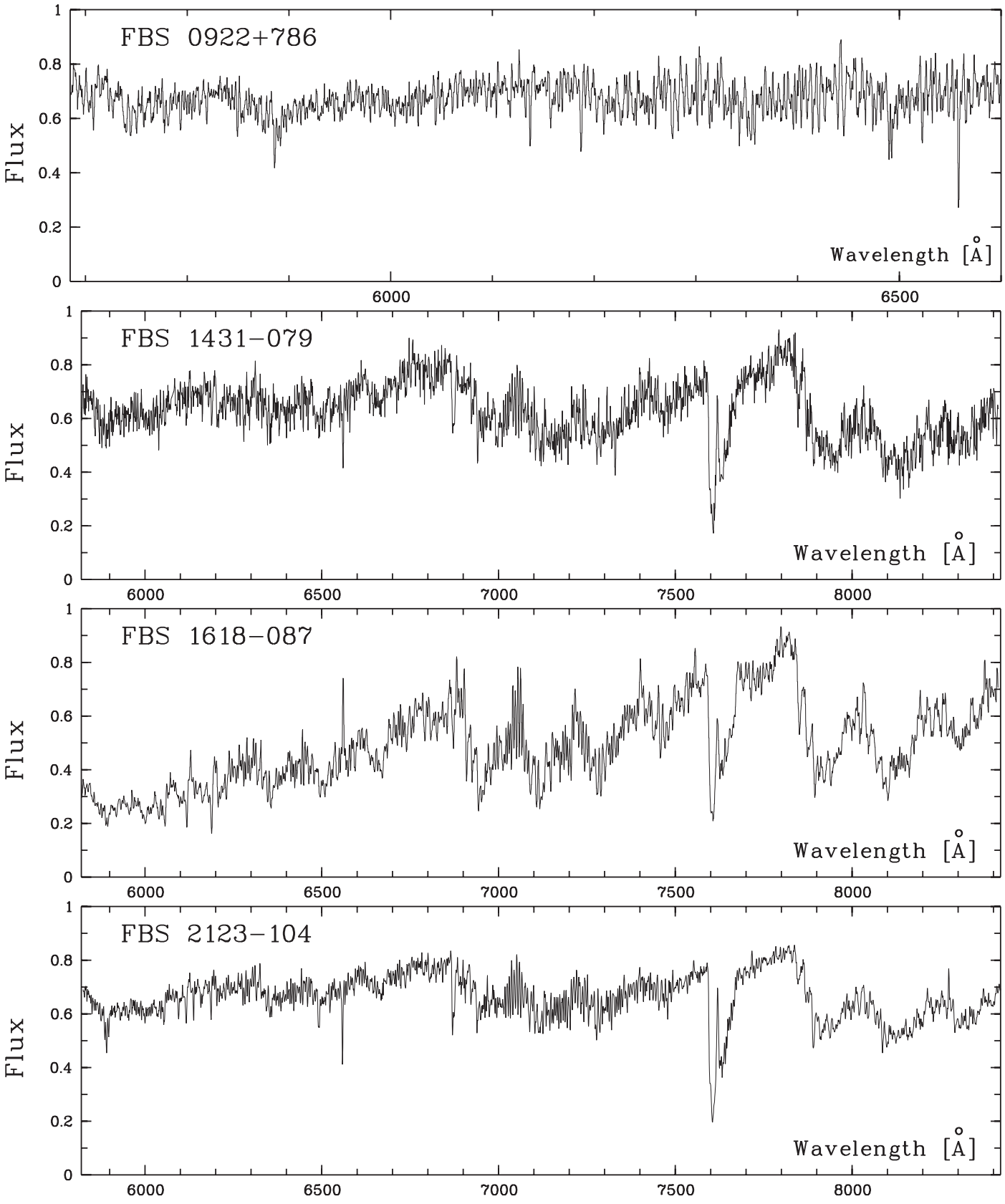
FBS 0922+786
FBS 1431−079
FBS 1618−087
FBS 2123−104
Flux
Wavelength [Å]
0
0.2
0.4
0.6
0.8
1
6000
6500
7000
7500
8000

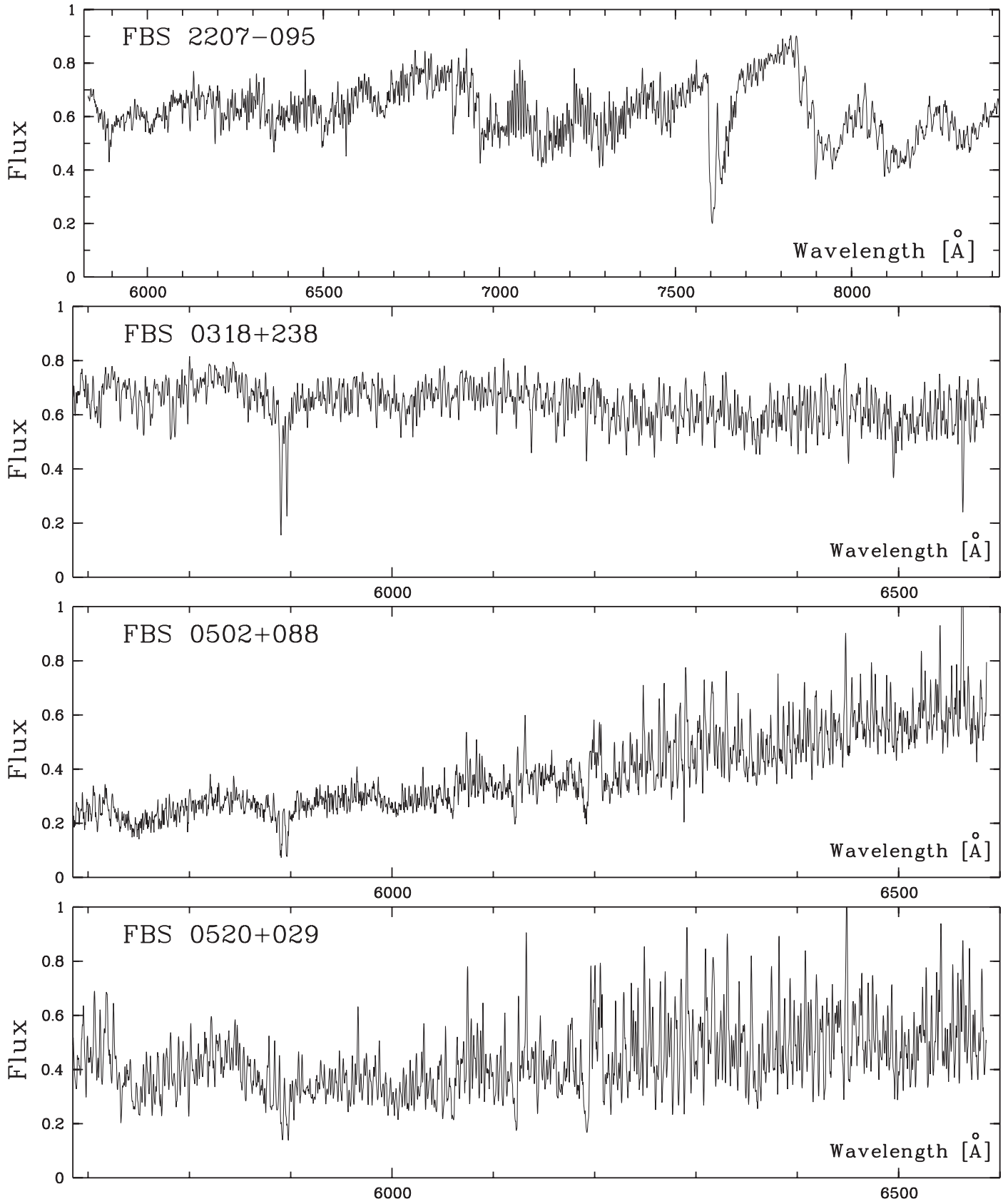
FBS 2207−095
FBS 0318+238
FBS 0502+088
FBS 0520+029
Flux
Wavelength [Å]
0
0.2
0.4
0.6
0.8
1
6000
6500
7000
7500
8000

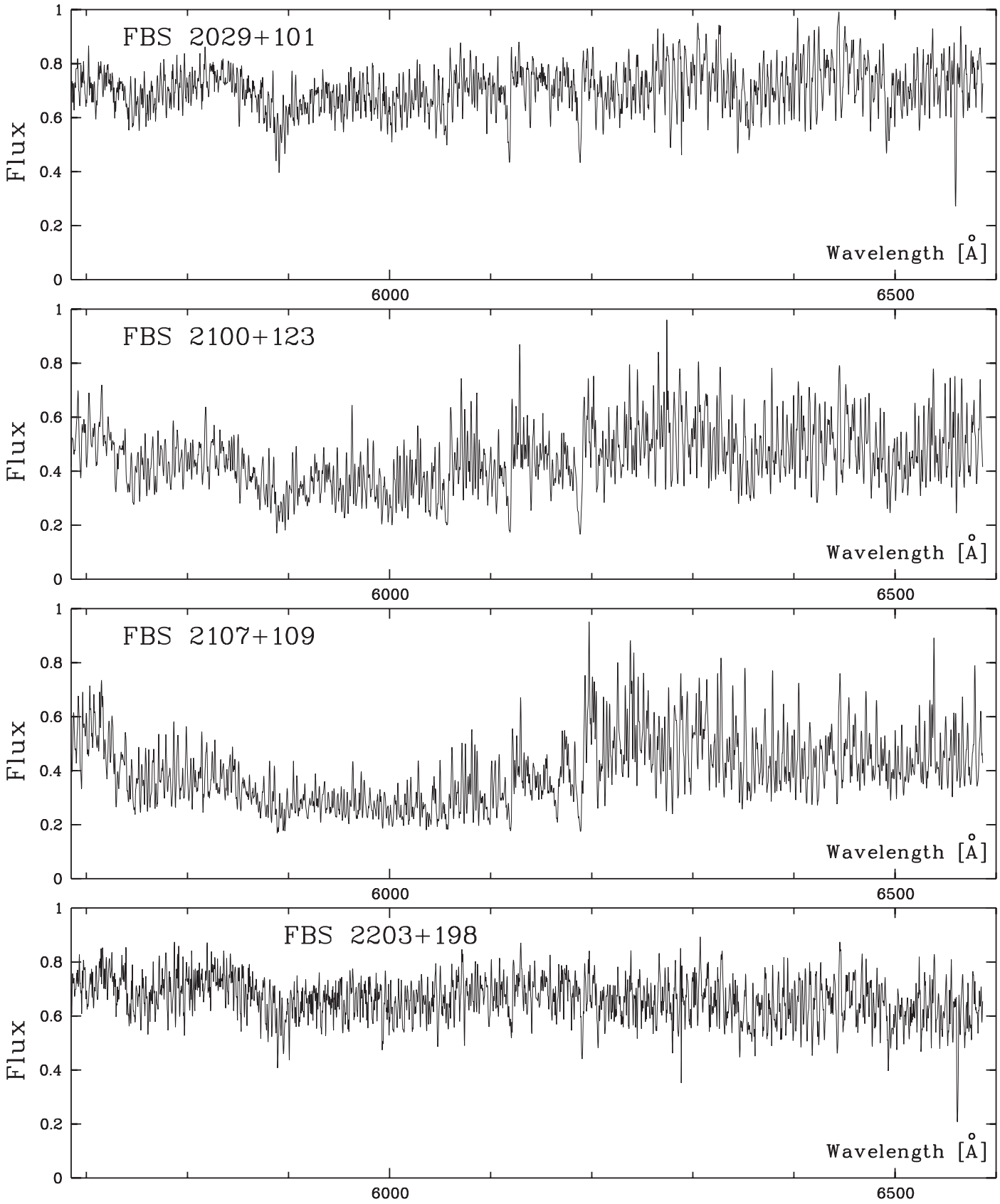
FBS 2029+101
FBS 2100+123
FBS 2107+109
FBS 2203+198
Flux
Wavelength [Å]
0
0.2
0.4
0.6
0.8
1
6000
6500

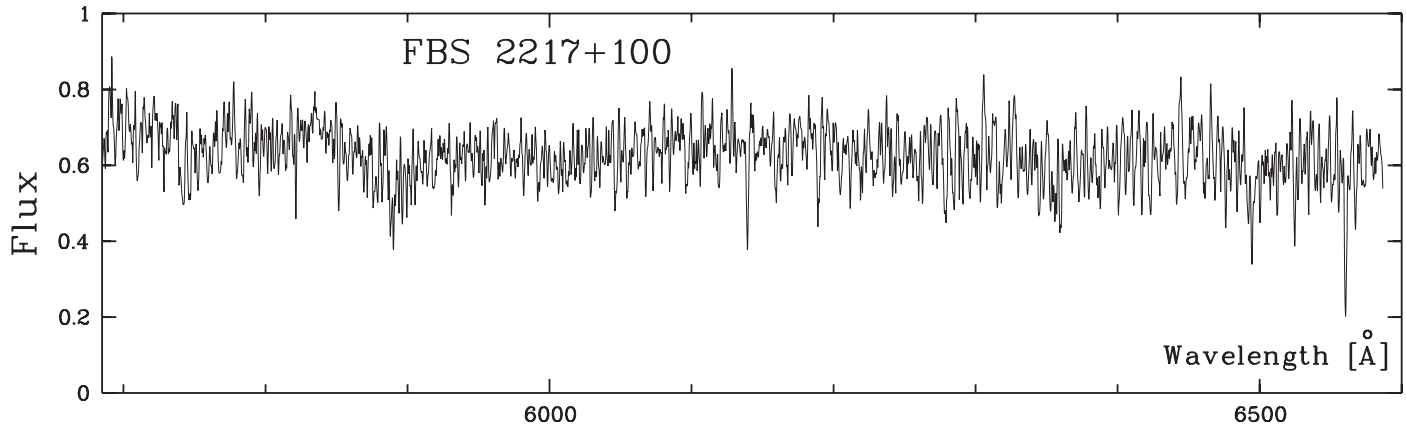
FBS 2217+100
Flux
Wavelength [Å]
1
0.8
0.6
0.4
0.2
0
6000
6500

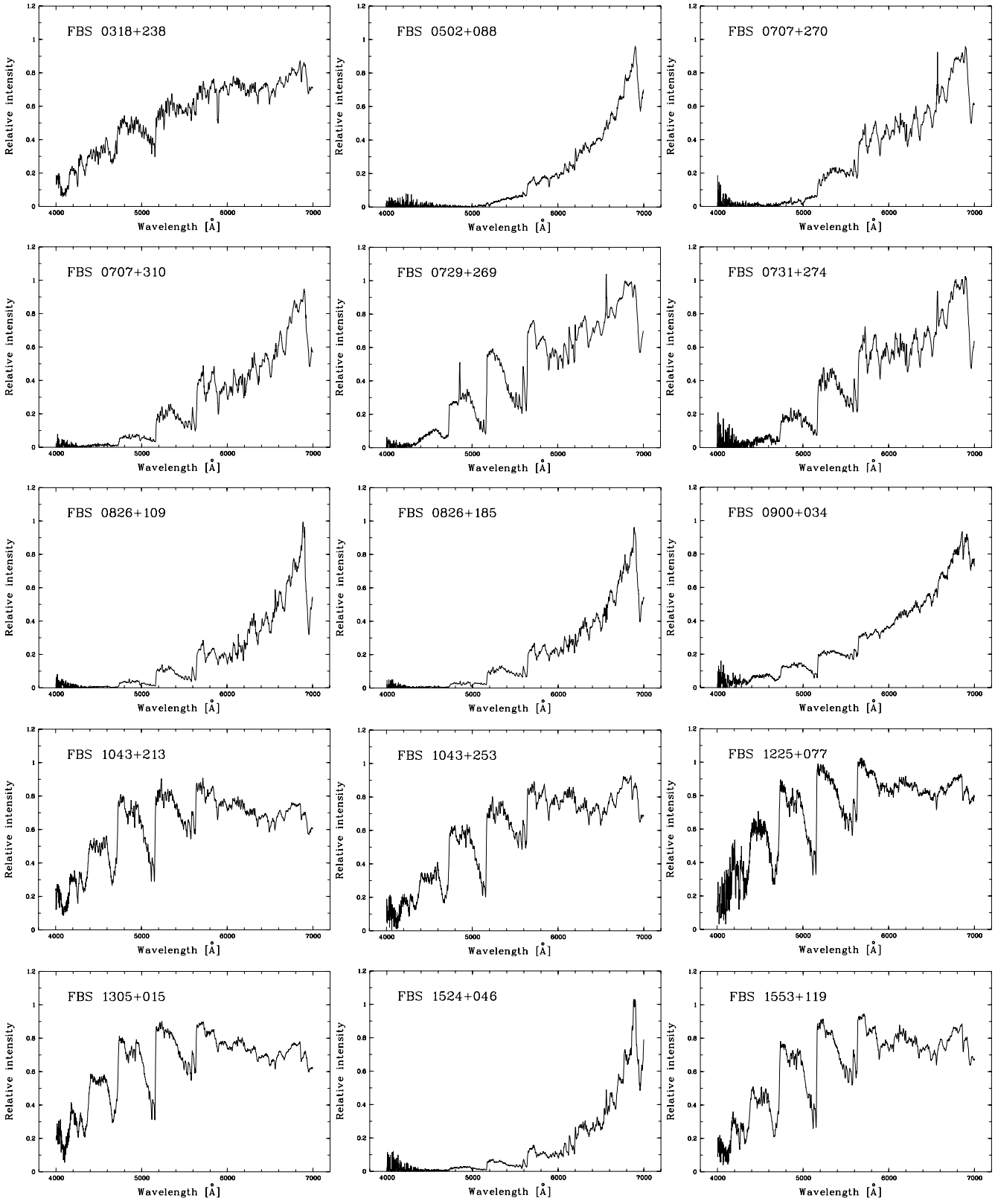
FBS 0318+238
FBS 0502+088
FBS 0707+270
FBS 0707+310
FBS 0729+269
FBS 0731+274
FBS 0826+109
FBS 0826+185
FBS 0900+034
FBS 1043+213
FBS 1043+253
FBS 1225+077
FBS 1305+015
FBS 1524+046
FBS 1553+119
Relative intensity
Wavelength [Å]

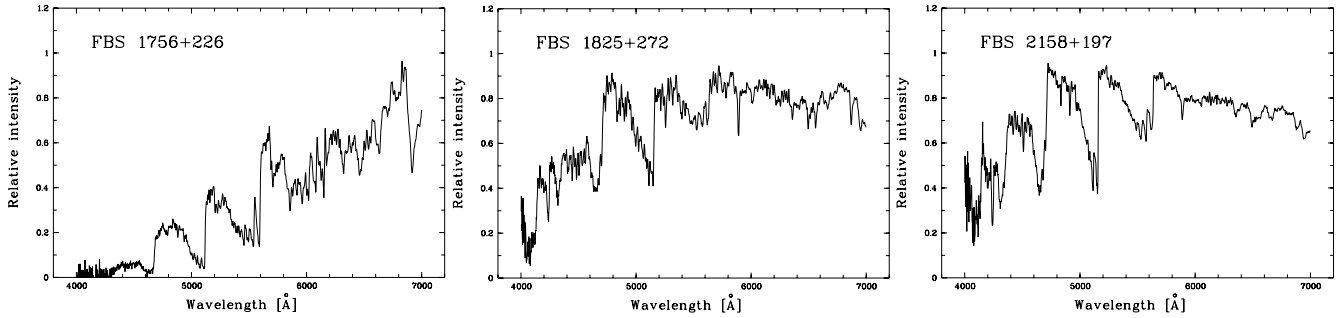
FBS 1756+226
FBS 1825+272
FBS 2158+197
Relative intensity
Wavelength [Å]